V.J. Levin [1], R.J. Stepan [1] and A.I. Leonov [2]

Evaluating Tackiness of Polymer Containing Lubricants by Open-Siphon Method: Experiments, Theory and Observations

July 11, 2007

[1] Functional Products Inc., 8282 Bavaria Road, Macedonia, OH 44056, USA
Email: vlevin@functionalproducts.com or rstepan@functionalproducts.com
[2] Department of Polymer Engineering, The University of Akron, Akron, OH 44325-0301, USA
Email : leonov@uakron.edu

Abstract

This paper investigates tackiness of several lubricant fluids using familiar open siphon technique. In these experiments, evacuated sucking tube withdraws vertical free jet of liquids from a jar with a free surface. Dilute solutions of polyisobutelene (PIB) of different molecular weights and polymer concentrations in lubricating fluids, as well as the blends of PIB with ethylene-propylene copolymer were used in these experiments. Time dependences for the length and shape of free jet, and flow rate in the process were recorded in the experiments for several values of vacuum pressure in sucking tube and for several lubricant fluids. The *tackiness* of lubricant fluids was quantified by the ultimate length of free jet just before it breaks up. Experimental data were described and interpreted by a non-steady extension of an earlier stationary theory, modified for very dilute polymer solutions. Several specific phenomena were observed in the experiments, such as solvent exudation out of extended jet, maximum on the time dependence of flow rate during the process, maximum of tackiness for solutions of blends of tackifier and non tackifier, and a two-phase flow in sucking capillary.

1. Introduction

In many industrial applications the lubricating oil must not drip or mist from the bearings. It can be practically achieved by increase in cohesion energy of lubricant fluid, which prevents its atomization, while keeping the oil viscosity as low as possible, which prevents the liquid from excess in wasting energy. Just the texture of such optimal lubricating oil should be stringy, preventing oil loss and increasing lubrication time for machineries where the oil waste is a problem. To satisfy the above industrial needs, the lubricating industry has invented and utilized special types of lubricating oils containing tackifiers, which are solutions of polymers in oil. Till the present, typical applications of tacky lubricants are limited to high molecular weight polyisobutelene (PIB) dissolved in petroleum oil.

For polymer solutions to be tacky, the polymer chains should have a capacity to extend. It means that the tacky lubricants fluids should have elastic properties or to be viscoelastic liquids. To be less viscous and cheaper, they should also be very dilute polymer solutions in lubricant oils. It is well known that the viscoelastic properties of polymer solutions depend on polymer concentration and several molecular parameters of polymer determined by its chemical structure [1-3]. The most important parameters are the polymer molecular weight (and to some extend, the molecular weight distribution) and the flexibility of polymer chains; the latter being responsible for uncoiling of chains with smaller Kuhn segment, or orientation of chains in the direction of extension for more rigid chains. Another important parameter of a tacky polymer solution is the viscosity of the base solvent. Preparation and testing of various lubricants with enhanced tackiness is in high demand for lubricant application. Yet to the best of the author's knowledge, there are no studies of the tackiness phenomena in lubricant polymer solutions.

The present paper investigates the tackiness of very dilute solutions of polymer containing lubricants using the well-known open siphon method introduced and described in paper [4] (see also the monographs [5,6]). In this method, elastic liquids are vertically withdrawn out of a jar by a vacuum connected capillary. The suction pulls upwards a tacky liquid out of the jar forming a free jet (string). More tacky fluids draw a longer jet in air than less tacky ones, whereas non-tacky fluids are not drawn upwards at all. Basic experiments and theory analyzing the open siphon phenomena on example of water solutions of polyethylene oxide (PEO) were initiated in paper [7], using a viscoelastic approach. Prokunin [8], utilizing the idea of relaxation liquid-solid transition [6], developed the theory further, considering the free jet withdrawn from viscoelastic solution, as a pure elastic gel. He found a good comparison between his calculations and experiments of paper [7]. These results were later reviewed in monograph [6]. The experimental and theoretical results in papers [7,8] described, however, only the stationary processes of withdrawal of free viscoelastic jets by a rotating drum, where the constant speed of withdrawal and the flow rate of the fluid were controlled by the speed of drum rotation. Additionally, the experiments [7,8] were conducted on concentrated water solutions of very high molecular weight PEO with polymer volume concentration

0.5%. Thus to analyze and describe the withdrawal of viscoelastic jets of very dilute polymer solutions in the non-stationary sucking open siphon process, the previously developed stationary theory [6, 8] has to be modified.

It should also be mentioned that the problem of withdrawal of viscoelastic liquids seems similar to the withdrawal of viscous liquids by a vertically moving flat (or cylindrical) plate. In this problem a viscous liquid forms a thin layer near the rigid plate under the action of viscosity, gravity and surface tension. The solution of the problem mastered by Landau and Levich [9, 10] uses a matching condition between viscous flow and static meniscus. In spite of seeming similarity between these two problems, withdrawing of polymer solutions from a free surface is more complicated because the radius of extendable jet, varied with height is a priory unknown.

The paper is organized as follows. Section 2 describes the experimental set up, procedures and the fluids used in experiments. Section 3 introduces some basic facts of viscoelasticity known for polymeric liquids. Section 4, using a quasi-steady approach, modifies the theory [6,8] in the non-steady case of the open siphon with sucking devise, and applies it to very dilute polymer solutions. Section 5 discusses the quantitative experimental findings and describes the data using the theory of Section 4. Section 6 applies the open siphoning method for evaluations of tackiness in two different lubricant oils. Concluding remarks are given in the last Section 7 of the paper.

2. Experimental set up, procedures and fluids

The experimental device used for testing tackiness of lubricating fluids is similar to those described in Refs.[4,5]. The set up is explained in Fig.1 where the glass tube (capillary) with inner diameter of 1.58 mm and length 120 mm is connected to the common vacuum equipment. We used in the experiments three values of vacuum pressures p_v equal to 68, 77.3 and 84 KPa. The graduated glass cylinder ("jar") filled with a tested fluid was of inner diameter 28mm and height 190mm. To quantify the jet profiles we used the Konica Minolta A4 camera and computer, equipped with Adobe Photoshop CS2 program for enlarging pictures of the jet.

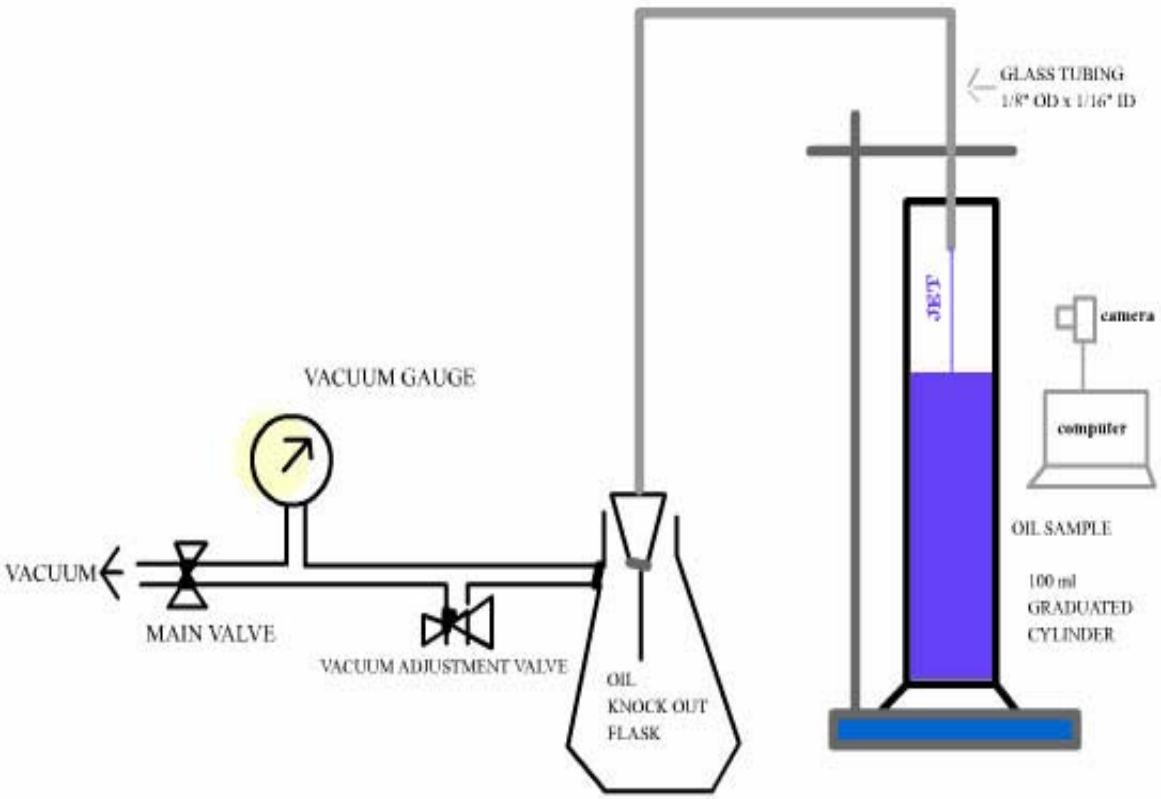

FIGURE 1

Experimental set up for testing tackiness.

The experimental procedure was as follows. The capillary was lowered in the jar filled with the tested liquid, so the lower sucking end of capillary was initially below the liquid surface. Then the capillary was held in this position during the test. The suction pulled the liquid into the capillary and lowered the level of liquid in the jar. The experiment began at the moment when falling liquid surface in the jar reached the lower end of the capillary. Starting from this moment a free jet of a tacky liquid was formed. The siphon draws down the level of liquid in jar, increasing the length of free jet and making it progressively thinner. Flow rate q measured by graduated jar-cylinder was dependent on applied vacuum; the higher the vacuum the higher was the flow rate. At small flow rates the jet was broken, at large enough flow rate the jet lost its axial symmetry and the flow rate oscillated with time. We chose the above range of vacuum

pressure to prevent breakage and high oscillation. But even in this range we observed some sporadic oscillation of the jet. Because of this we repeated each measurement three times, recording an average value for calculations. The photo of the jet shown in Figures 2a,b demonstrates a very characteristic feature of the jet, a relatively large viscoelastic meniscus near the free surface. Some traces of instability are also seen in these Figures.

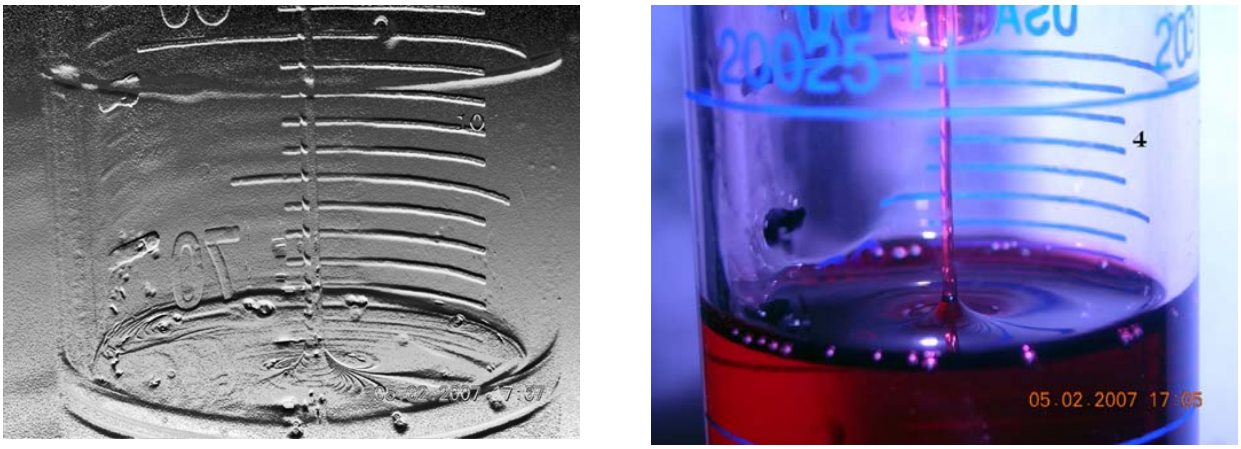

Fig.2a,b. Photographs of free tacky jets for 0.025% PIB solution in lubricant oil.

We measured the size and shape of the jet by taking photographs every 25 seconds after the beginning of withdrawing. The maximum length of the free jet supported by the vacuum is recorded as a "string length" or *tackiness*. Photos were enlarged in the computer using Adobe Photoshop CS2 program. Using the printed pictures we measured the jet radius r at different distances z from the liquid surface and at different flow rates q. Special attention were given to measurements of parameters of meniscus which appears at the moment of disconnecting the capillary and fluid. These are the radius of meniscus R and radius of jet r_0 at the top of meniscus, measured at different flow rates q.

In the main part of experiment discussed in Section 5, we used 0.025% (weight) PIB solution with viscosity average molecular weight $M_\eta = 2.1\times10^6$ [11] in the oil ISO 68, which has viscosities $\eta_s \approx 0.138$, 0.0585, and 0.0073 Pa·s at 20, 40 and 100ºC, respectively. Viscosities were measured by using capillary ASTM D 445 method. The

density ρ_s of this oil at 25ºC is equal 0.86 g/cm^3. Surface tension γ_s at 20º is equal to 2.7 Pa$\cdot$cm [12].

In other, industrially driven experiments, whose results are briefly discussed in Section 6 we also used various PIB with $M_\eta = 0.9\times10^6,\ 1.6\times10^6,\ 4.0\times10^6$, with weight concentration varied from 0.005% to 0.12%, dissolved in the mineral oil with viscosity η_s at 40ºC equal to 0.068 and 0.022 Pa$\cdot$sec. These are the standard ISO Grades ISO 68 and ISO 22 oils widely used in lubrication industry. Solution of ethylene propylene copolymer with molecular weight about 200,000 was also used. Polymers were granulated and then dissolved in oil in a glass container on hot plate with low-shear agitation. The time of dissolution was approximately 48 hours.

3. Viscoelastic effects in withdrawal of tacky lubricants

As viscoelastic polymer dilute solutions, the tacky lubricant liquids can be characterized by three basic parameters, solvent viscosity η_s, the polymer volume concentration c, and relaxation time θ. It is well known that at the very small concentrations of polymer additives, the viscosities η of polymer solutions practically coincided with those η_s for the mineral oil solvents. Nevertheless, adding very small concentrations of PIB into the mineral oil dramatically increases the relaxation time θ of the solutions.

Elastic liquids, by their reply to external actions, are in an intermediate position between viscous liquids and elastic solids. They behave as viscous liquids at low rates of external actions and as elastic solids when these rates are high. This type of behavior is commonly estimated by the non-dimensional Weissenberg number We. In extensional flows, including the problem of withdrawal, it is presented as [6]:

$$We = \theta \cdot \dot{\varepsilon}\,. \tag{1}$$

Here $\dot{\varepsilon}$ is the elongation rate, i.e. velocity gradient in the direction of extension (withdrawal). When extensional rate is low $We << 1$ a viscoelastic liquid behaves as a viscous one. In the opposite case when $We >> 1$, the solid-like properties of viscoelastic liquids dominate and they behave as elastic solids.

Along with well known basic facts, many elastic liquids display a fast transition from the liquid-like to the solid-like behavior when passing through a certain threshold We_c in the Weissenberg number. This phenomenon called the *fluidity loss*, has been well documented for narrowly distributed polymers and treated as a *relaxation transition* (e.g. see the mograph [6] and references there). The underlying physics of this transition is that the highly oriented polymer molecules in certain flows create physical cross-links which cause effective gelation of polymers and ceasing the flow. In case of withdrawal of dilute polymer solutions the fluidity loss effect assumed in Refs. [6, 8] could also be caused by an increase in polymer concentration in intense extensional flows near the axis of extension. This might happen because the fluid trajectories in extensional flows cause the polymer macromolecules closely approach each other.

4. Theoretical model

In order to make clear the basic physics of processes in the withdrawal of tacky lubricants we now discuss modification of the theoretical model developed in Refs.[6-8]. This modification is based on the following assumptions: (i) the effect *of fluidity loss* plays a dominant role in the jet withdrawal, (ii) the *inertia phenomena* are negligible in dynamics of polymer jet withdrawal, and (iii) *exudation of solvent* out of withdrawn jet is important in case of dilute polymer solutions.

The first and second assumptions have been employed and proved valid in paper [8] on example of 0.5% water solution of very high molecular weight PEO. In case of dilute polymer solutions the validity of these assumptions is a priori unknown. Neglecting inertia effects allows one to extend the stationary theory to the non-stationary case, using the quasi-steady approach. The third assumption comes from observations of withdrawn lubricant jets, and plays important role in the following modeling.

To develop a formal model we introduce the vertical coordinate z, which coincides with the jet centerline and is counted off the moving free surface (Fig.3). So the origin $z = 0$ is located at the free surface, and the upper coordinate $z = l(t)$ at the capillary entrance indicates the length of visible jet at time t. It is convenient for theoretical treatment to roughly separate the whole domain of the liquid flow in the three regions:

region 3 $\{z < 0\}$ located under free surface, *meniscus region* 2 $\{0 \le z \le R(t)\}$ located from the free surface up to the end of meniscus, and the *region*1 of free jet motion $\{R(t) \le z \le l(t)\}$ (see Fig.3). Here the functions $R(t)$ and $l(t)$ are unknown and have to be determined. Basic flow effects which occur in the three regions of flow could be qualitatively described as follows [6-8].

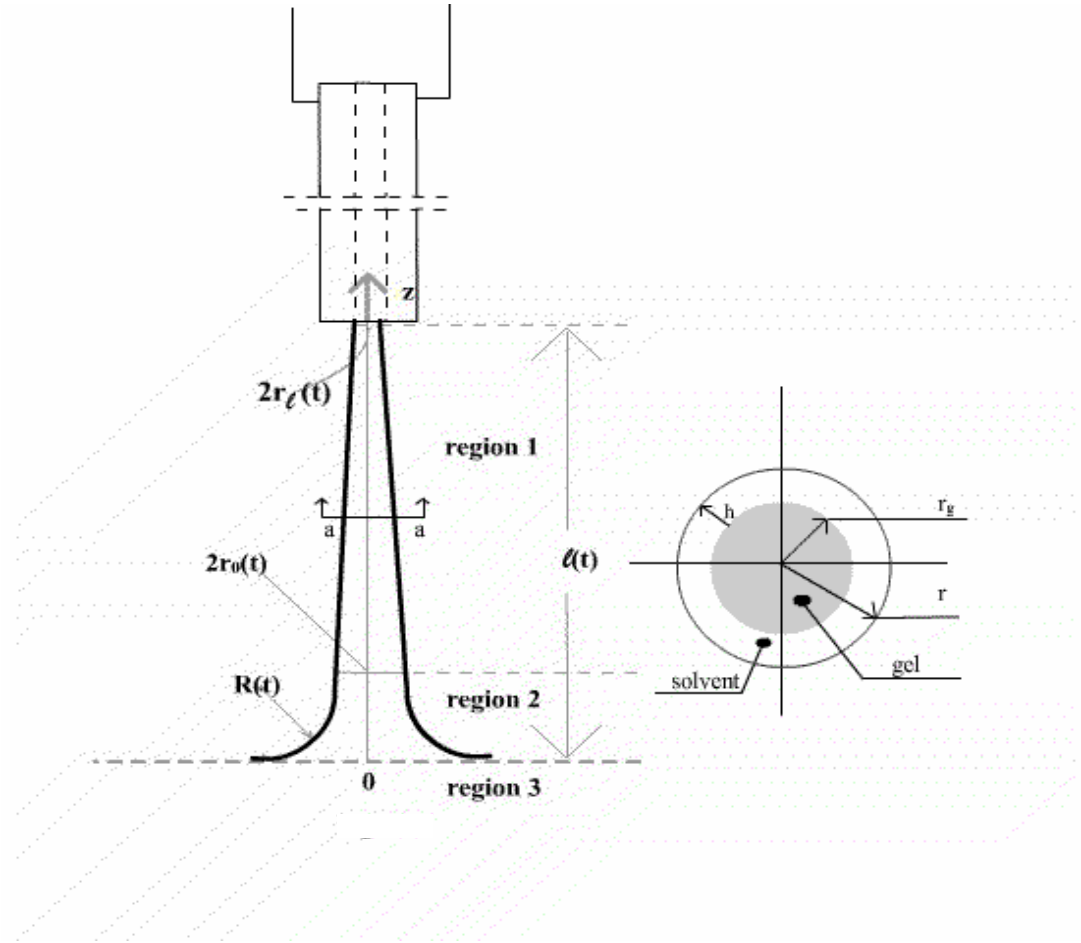

Fig.3. Schematics of jet withdrawal

In the region 3 the sucking effect from capillary causes a specific extensional flow. This flow, slowly changing in time, looks like an effective undersurface jet which narrows from the bottom to the surface. Therefore the vertical velocity of jet and the characteristic extensional velocity gradient $\dot{\varepsilon} \approx dV / dz$ are increased when approaching the surface from below. Substituting this value of $\dot{\varepsilon}$ into (1) explains the increase in the Weissenberg number, which might cause the relaxation fluid-solid transition. It was speculated in Refs. [6,8] that the complete relaxation transition happens in the region 2,

where still viscoelastic polymer solution forms a free jet which is squeezed under additional action of surface tension. In the region 1 the free jet can be treated as an elastic gel swollen in solvent, which has a string-like shape, and is under the action of extensional force, gravity and surface tension.

For describing the free jet behavior in the region 2 we will use a semi-empirical approach [6-8] instead of analyzing complicated viscoelastic flow in the regions 2 and 3. This approach roughly approximates the shape of static meniscus by the expression:

$$r(z,t) \approx r_0 + R - \sqrt{R^2 - (R-z)^2} \qquad (0 \le z \le R). \tag{2}$$

Here $R(t)$ is the maximum height of meniscus and $r_0(t)$ is the initial (maximal) radius of the free jet. The geometrical picture of this approximation is sketched in Fig.3, although the circle of radius R with a horizontal tangent at $z = 0$ surely cannot smoothly touch the meniscus surface at $r = r_0$. In spite of its very approximate character, formula (2) allows describe some critical phenomena at low flow rates and also interpret the measurements of jet radius near the free surface $z = 0$.

In spite of very dilute character of polymer solutions in our study, we assume that the analysis of jet behavior in the region 2 is identical to that in Refs. [6,8]. Utilizing dimensional and geometrical arguments, this approach yields the relations:

$$R = \alpha(q\theta)^{1/3}; \;\; r_0 = \beta(q\theta)^{1/3} \;\; \left(S_0 = \pi r_0^2 = \pi\beta^2(q\theta)^{2/3}\right), \tag{3}$$

$$\sigma_0 \approx \rho g m R + 2\nu\gamma / R = \rho g m \nu r_0 + 2\gamma / r_0 . \tag{4}$$

Here σ_0 is the stress at the initial jet radius r_0, $q(t)$ is the flow rate, θ is a characteristic relaxation time, ρ and γ are the density and surface tension of solution, respectively, whose values will be evaluated by the corresponding values ρ_s and γ_s mentioned for solvent. Also in (3) and (4), α and β are numerical parameters, whose values are estimated by fitting, and

$$\nu = \alpha / \beta, \qquad m = m(\nu) = \nu^2[2/3 + (1+1/\nu)^2 - (\pi/2)(1+1/\nu)]. \tag{5}$$

The first and second terms in identical expressions (4) for stress σ_0 describe respectively the contributions of weight and surface tension of the liquid column in the meniscus area 2. The bottom stress σ_0, being due to (4) a function only of R (or r_0), has a

minimum at $R = R_c$ (or r_{0c}). The minimum value of initial stress $\sigma_{0\min}$ and corresponding values of R_c (or r_{0c}) and q_c are given by:

$$\sigma_{0\min} = (c_1 \rho g \gamma)^{1/2}, \quad R_c = [c_2 \gamma/(\rho g)]^{1/2}, \quad r_{0c} = [\hat{c}_2 \gamma/(\rho g)]^{1/2} \quad \theta q_c = [c_3 \gamma/(\rho g)]^{3/2}$$
$$c_1 = 8m\nu, \quad c_2 = 2\nu/m, \quad \hat{c}_2 = 2/(\nu m), \quad c_3 = c_2/\alpha^2 \qquad (6)$$

Here numerical parameters $c_1, c_2, \hat{c}_2$, and c_3 are calculated using (5). The values of R_c (or r_{0c}) and q_c have a physical sense of critical parameters, below which the jet structure does not exist [6, 8]. Remarkably, these values depend only on the equilibrium physical parameters of the fluid, its density ρ and surface tension γ, being independent of the withdrawal conditions and viscoelastic constants of liquid.

In order to analyze the jet behavior in the region 1 we mention first unusual flow phenomenon in the sucking tube (capillary), recorded in experiments and shown by a photograph in Fig.4.

Fig.4. Photographs of two-phase motion of jet in capillary.

Here the jet entered the tube with considerably less diameter than the inner capillary diameter, and at higher vacuum, seemingly continued its extending up to the upper capillary end. It means that instead of visible jet length $l(t)$ introduced above, the total jet length $L(t)$ at higher vacuum should be considered as the real dynamic variable, where

$$L(t) = l(t) + l_T, \tag{7}$$

and l_T is the sucking tube length.

In case of withdrawal of dilute polymer solutions, an additional effect of *strain induced exudation of solvent* should also be taken into account. Although the kinetics of this process is unknown, the flow of a thin film of solvent covering the gelled jet, swollen in the solvent, is guessed to be much the same as in case of thin film withdrawn from a vessel by a vertically wall moving upwards, i.e. controlled by the vertical drag speed, viscosity, gravity and surface tension [9].

To take into account solvent exudation we introduce the *two-phase model* of jet sketched in the box of Fig.3, where the actual radius r of jet is represented as the sum of actual radius r_g of the gelled jet and the precipitated film thickness h, i.e. $r = r_g + h$. At any radius r, we roughly treat the core of the swollen jet with radius r_g as an elastic solid with large deformations, whereas the peripheral thin film of solvent with thickness h as a viscous liquid. We neglect the contribution of the solvent film in axial stretching stress. Yet we consider in this two-phase model the local surface tension effect as acting on the total radius r.

We then roughly hypothesize that the film thickness h depends only on time. Using also the scaling argument, we assume that $h \approx \xi r_0(t)$ where $\xi = \xi(q_c / q) \le 1$ is a positive increasing function, and $r_0(t)$ is the maximum radius of the jet at time t (see Figure 3). Thus this two-phase approach yields the kinematical relation:

$$r = r_g + h(t) = r_g + \xi(q_c / q(t)) r_0(t). \tag{8}$$

Neglecting a possible effect of the solvent film in the region 2, the dependence $r_0(t)$ will be calculated at the end of this Section, using the kinetics of jet withdrawal and analyzing effects in the region 2. The function $\xi(q_c / q(t))$ will be proposed in the next Section.

We now use the above assumption that in the region 1, the core of gelled jet behaves as a weakly cross-linked purely elastic solid with a very low elastic modulus μ and very large elastic strain λ ($>>1$). We employ in the region 1 slightly inhomogeneous quasi-1D common approach, almost the same as in the homogeneous extension (e.g. see [6,8]). Then using (8) yields:

$$\lambda = \lambda_0 (r_{0g} / r_g)^2 = \lambda_0 [(1-\xi) r_0 / (r - \xi r_0)^2] . \tag{9}$$

$$\sigma \approx (\mu / n) \lambda^n - \gamma / r \qquad (\ (n > 1) . \tag{10}$$

Here λ and σ are stretch ratio and stress, respectively, n is a numerical parameter characterizing a specific elastic potential [8], and λ_0 is an extensional stretch ratio attributed to the liquid-solid transition in the region 2.

The non-inertial momentum and mass balance equations, averaged over the jet cross section can be written in the form similar to those used in Refs. [6, 8]:

$$d / dz \left(\sigma S_g - 2\gamma \sqrt{\pi S} \right) = \rho g S \quad (S = \pi r^2,\ S_g = \pi r_g^2) \tag{11}$$

$$uS = u_g S_g + u_f S_f = q(t) \quad (S_f = S - S_g) \tag{12}$$

Here S, S_g and S_f are the total, occupied by gel and by solvent film cross-sectional areas, respectively, r is the actual radius of jet, u, u_g and u_f are the total, gel and solvent film vertical velocities, respectively. Note that if $u_g \approx u$ then $u_f \approx u$ either. It means that the solvent film is drawn upwards with the same speed as the gel.

Substituting (9) and (10) into (11) yields the following solution of stress-strain problem (4)-(6) described by the two-phase model:

$$\sigma = G_0 \left(\frac{r_0 (1-\xi)}{r - \xi r_0} \right)^{2n} - \frac{\gamma}{r}, \qquad z - R = \frac{n-1}{n} \cdot \frac{G_0}{\rho g} \left[\left(\frac{r_0 (1-\xi)}{r - \xi r_0} \right)^{2n} - 1 \right] - \frac{\gamma}{\rho g} \left(\frac{1}{r} - \frac{1}{r_0} \right) \tag{13}$$

$$(G_0 = \sigma_0 + \gamma / r_0)$$

Formulae (13) in the limit $\xi \to 0$ have the same form as in Refs. [6,8]. Parameters r_0, S_0, σ_0, G_0 in (8) are slow functions of time. They represent the boundary values of respective variables at the level $z = R$. These boundary values should be determined by matching the behavior of liquid in the regions 1 and 2. Also the function $\xi(q_c / q_0)$ is a slow function of time. As soon as these values are found, the jet profile and the stress

distribution along the jet in the region $(R < z < L(t))$ are determined for any time instant from relations (13).

We now consider the long jets with such large values of z that the surface tension effects on the stress are negligible as compared with the gravity. For these values of z the solution of (13) of the withdrawal problem has the asymptotic form found in Refs. [6, 8]:

$$\sigma \approx \rho g\left(\frac{n}{n-1}z + \frac{m(c-1)}{c}R\right) \qquad (c = m(n-1)/n) \tag{14}$$

Here the numerical parameter c is again expressed via α and β using relations (12). When the first term in bracket in (14) dominates, the simplified expression will be used:

$$\sigma \approx \rho g z n/(n-1) \quad (z >> R). \tag{15}$$

The above formulae (9)-(15) have been obtained in [8] for stationary withdrawal problem in the limit $\xi \to 0$ using the non-inertial approach. In [8], the characteristic sizes R and r_0 of the meniscus as well as the flow rate q have certain constant values. In the non-steady case of jet withdrawal under study, these formulae are still valid because of a slow non-inertial approach, although the basic kinematical variables of the process, the length of withdrawn jet $L(t)$ and the flow rate q are now some functions of time t. To determine these functions $L(t)$ and $q(t)$, we will use two additional physical conditions.

The first, kinematical condition evident from Figures 1 and 3 is:

$$q(t) = A \cdot dL/dt. \tag{16}$$

Here $A = \pi r_j^2$ is the cross-sectional area of the measuring cylinder (jar). Equation (16) shows that the change in length of the withdrawn jet is caused by the decrease of the liquid level in the jar.

The second, dynamic condition describes the dependence of flow rate on the pressure drop for the liquid flow in the sucking capillary. If there were a back gel-fluid transition in the sucking capillary, this dependence must be described by the well-known linear Poiseuille formula. However, this back gel-fluid transition was never observed in the sucking capillary. Instead, a very complicated two-phase flow shown in Fig. 4, occurs there. It seems that at the highest vacuum, the jet continues being extended in the sucking capillary up to its very end. After that the jet brakes down of the two-phase liquid-air mixture in the adjacent tube. At lower values of vacuum, this braking process happens in

the sucking capillary. Because of relative slowness of withdrawal process, this typically viscous, complicated flow could still be described by a linear hydraulic type relation between the pressure drop and flow rate:

$$q \approx k(\sigma_{\text{v}} - \sigma_L) \quad (k = const), \quad \sigma_{\text{v}} = p_a - p_{\text{v}}. \tag{17}$$

Here σ_{v} is the pulling stress due to vacuum, p_{v} and p_a are the absolute vacuum and atmospheric pressures, respectively, and σ_L is the acting elastic stress in the jet at the level $z = L(t)$. The constant k of dimensionality $cm^3/(Pa \cdot \sec)$ describes the hydraulic resistance of jet at the end of sucking capillary. It should be evaluated by comparison of the theory with experimental data.

Determining σ_L from asymptotic formula (15) at $z = L(t)$ and substituting it along with (17) into (16) yields the kinetic equation describing the time evolution of $L(t)$:

$$dL/dt + sL = sL_u. \tag{18}$$

Here s is a parameter of dimensionality of 1/sec, and L_u is the ultimate length of the whole jet achievable with a given vacuum; these parameters being described as:

$$s = \frac{n}{n-1} \cdot \frac{\rho g k}{A}, \quad L_u = \frac{n-1}{n} \cdot \frac{\sigma_{\text{v}}}{\rho \text{g}} \quad . \tag{19}$$

Beginning with a time t_* where the asymptotic expression (15) is valid, solution of equation (18) is presented as:

$$L(t) = L_u \cdot \{1 - \exp[-s(t - t_*)]\} \quad (t \geq t_*). \tag{20}$$

Finally (16) and (20) yield the asymptotic expression for the flow rate:

$$q = s \cdot L_u \cdot \exp[-s(t - t_*)] \quad (t \geq t_*). \tag{21}$$

Formulas (19) and (21) will be used in the next Section for evaluation of parameters s and elastic constant of gel n. We should remind once again that these relations are reliable only after a certain time t_* elapsed from the beginning of the withdrawal process when the formula (15) is valid.

To describe the whole process from its very beginning one should employ numerical calculations using equations (3)-(5), (13), (16) and (17) where $z = L(t)$, $S = S(l(t)) \equiv S_l(t)$. Although these calculations can be performed relatively easily, the

problem is that the beginning of withdrawal is accompanied by a poorly understood two-phase motion of jet in capillary.

5. Experimental results with a 0.025% PIB solution; comparison with the theory

We first attract attention to the jet photographs presented in Figures 2a,b made with 5.3 magnification. There are clearly seen some horizontal ripples on the jet, which might be explained by secondary instability of solvent film exuded out of solvent. This instability well known for the liquid films flowing down on inclined surfaces [10], indirectly confirms the very fact of exudation of the solvent from the withdrawn jet.

With increasing time of withdrawing the diameter of jet dramatically decreases. The amount of liquid sucked from calibrated cylinder was measured every 5 sec. Using these data the time dependences of flow rate q ($cm^3/\sec$) were determined for different applied values of vacuum (Fig.5).

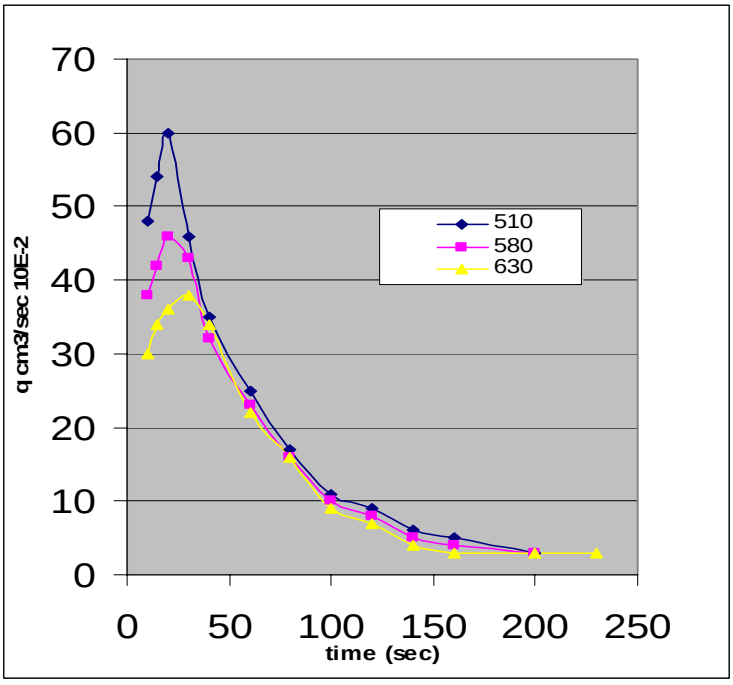

Fig.5. Time dependences of flow rate for different vacuum values (shown in the box). 0.025% PIB solution in lubricant oil.

At the beginning of withdrawing, flow rate q substantially increases in time and reaches a maximum at about 25 seconds from the beginning of withdrawing. The higher

the vacuum the higher is the q maximum and earlier its achieving. The possible explanation of the effect is as follows. The initial, just formed short jet is under action of surface tension and extension from sucking capillary. The action of surface tension squeezes the jet causing the increase in the flow rate. With increasing jet's length the gravity force comes into play and soon overcomes the surface tension effect, causing the decrease in flow rate.

Figure 6 demonstrates that the flow rate is proportional to the speed of change in the length of jet dl/dt $(= dL/dt)$. This is direct confirmation of evident kinematical relation (16) on the example of the highest used vacuum.

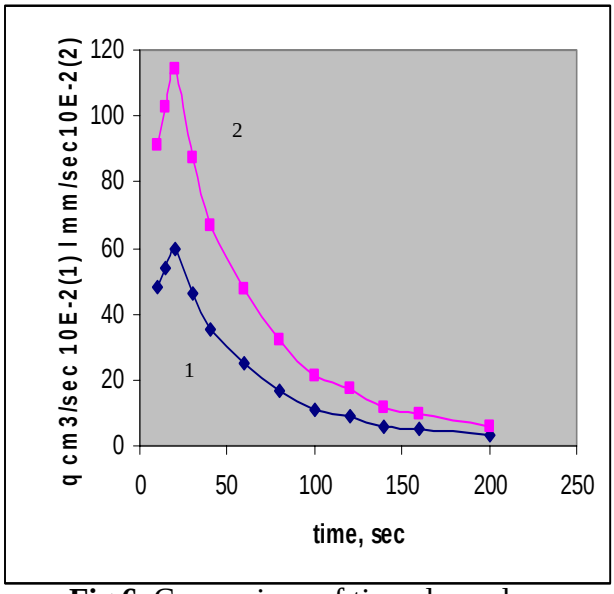

Fig.6. Comparison of time dependences of withdrawal rate $\dot{l}(t)$ (curve 1) and flow rate (curve 2) with vacuum value $\sigma_v = 32 KPa$ for 0.025% PIB solution in lubricant oil.

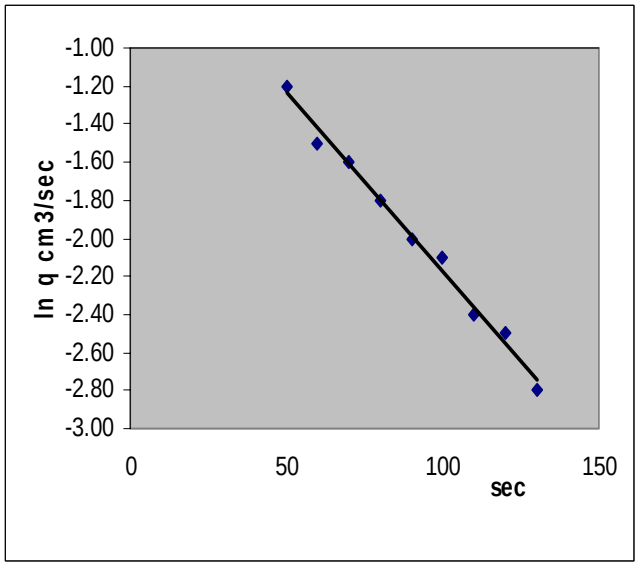

Fig.7. The decreasing branches time dependences of flow rate in Fig.5, represented in semi-logarithmic coordinates.

After passing through the maximum, the flow rate exponentially decreases. This effect, predicted by relation (21) is illustrated in Fig.7, where the time dependence of $\ln q$ is presented by a strait line with the slope equal to about -0.02 (1/sec). As seen from Fig.7 the decrease in applied (constant) value of vacuum also causes the decrease in flow rate, but after passing through the maxima the differences between curves with different

values of vacuum are negligible. Thus the data presented in Fig.7 illustrate the changes of average flow rate with time for three different values of vacuum.

Another important fact found in this paper is that independently of the vacuum values, all jets break at flow rate about $0.03\,cm^3/\sec$. The very existence of a lower critical value of flow rate is predicted by the fourth formula in (6). This fact will also be utilized in the following modeling.

Using the data presented in Fig.5 we choose on the decreasing branches $q(t)$ several flow rates, $q_1 = 0.35$, $q_2 = 0.25$, $q_3 = 0.20$ and $q_4 = 0.14\,cm^3/\sec$, corresponding to various time instances t_k. Making photographs at these t_k we measured the *jet profiles* corresponding to the flow rates q_k related to these instances t_k. In this region of flow rates, the measured jet profiles were well reproduced. Figure 8 presents these jet profiles as decreasing dependences of the jet radius r versus distance z from the liquid surface, up to the maximal visible jet length at those time instances t_k. In order to describe the jet profiles shown in Fig.8, we had to find along with the function $\xi(q_c / q(t))$ describing the thickness of exuded solvent in formula (13), three fitting parameters, numerical parameters ν related to the meniscus formulae (3)-(5), numerical parameter n describing the gel elastic potential (10), and parameter κ describing the stress-flow rate hydraulic relation (17).

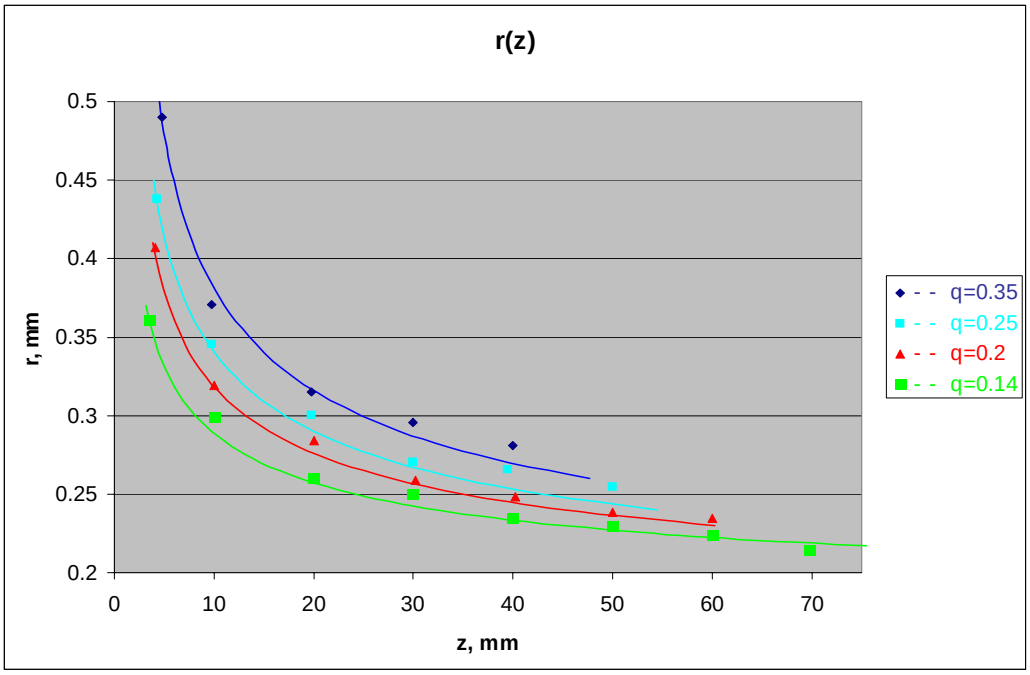

Fig.8. Jet profiles for several values of flow rate (shown in the box) established by photographing. 0.025% PIB solution in lubricant oil. Symbols – experimental data, solid lines – model calculations.

We first evaluate the parameters of meniscus. Starting with the highest value of flow rate $q_1 = 0.35\,cm^3$/sec, and using the abovementioned awkward procedure of meniscus approximation, we found the value $r_{01} \approx 0.49mm$ corresponding to the maximum flow rate q_1. All other values r_{0k} corresponding to different values of q_k have been calculated using the scaling formulae (3) as: $r_{0k} = r_{01}(q_k / q_1)^{1/3}$. As seen from Figure 8, the calculated data presented in Table 1, match well the experimental values. Then utilizing the fact that the lower critical value of flow rate $q_{0c} \approx 0.03cm^3/\sec$, we calculated the lower critical value of r_{0c} as $r_{0c} = r_{01}(q_1 / q_c)^{1/3} = 0.216mm$. Using this value, we employ expression (6) for r_{0c} and formula (5) for function $m(\nu)$ to yield the equation: $\nu m(\nu) \equiv \nu(0.0959\nu^2 + 0.429\nu + 1) \approx 137$. Solution of this equation is $\nu \approx 9.7$, and respectively, $m \approx 14$. Using these data we calculated the values of large meniscus radiuses $R = \nu r_0$, meniscus stress σ_0 due to (4), and the values of parameter G_0 in (13). These variables for above four profiles are presented in Table 1.

Elastic potential for the highly swollen elastic gel is unknown. It is characterized by the parameter n which is determined by a fitting procedure as follows. Consider the formula (19) for the total ultimate length L_u of the jet. Using the values of vacuum pressure reported in Section 2, we found that the corresponding values of pulling vacuum stress σ_v are: 32, 22.7 and 16 KPa, respectively. Consider the maximal value $\sigma_v = 32KPa$. Experimental results show that for this value of vacuum, the visible maximal length of withdrawn jet $l_u \approx 10cm,$ so the ultimate total jet value $L_u \approx 22cm$. Thus from the formula (19) for L_u we found $n \approx 1.062$.

Being unaware of strain induced exudation kinetics of solvent out of gel, we simply parameterize the function $\xi(q_c / q(t))$ by a power relation $\xi = (q_c / q)^a$. Fitting the jet profiles in Fig.8 with formula (13) we quickly found that $a \approx 1/2$, i.e. the thickness of the solvent film exuded out of gel under gel stretching is described as:

$$h = \xi \cdot r_0 = r_0 \sqrt{q_c / q} \ . \tag{22}$$

Simplicity of this result could indicate a fundamental physics of strain induced solvent exudation out of cross linked swollen gel. Revealing this physics is, however, outside the scope of this paper.

Using the above values of meniscus parameters and parameter n along with expression (22) we calculated jet profiles according to formula (13). Fig. 8 shows a good agreement between the calculations (solid lines) and experimental data (points).

We now consider the modeling of kinetics of long jet withdrawal, asymptotically described by formulae (16)-(20). Figure 6 discussed above, verifies the kinematical equation (16) on the example of higher pulling vacuum stress. Finally, the parameter k introduced in the hydraulic relation (17), is evaluated using (18) and value $s = 0.02\,\mathrm{sec}^{-1}$ as $k \approx 2.71 \times 10^{-5}\ cm^3/(Pa \cdot \mathrm{sec})$. Data of Figure 5 with the use of (20) and obtained values for s and L_u allow determine the time $t_* \approx 32\,\mathrm{sec}$ starting from which flow rate decays exponentially with time.

We now point out that the relaxation time θ could not be directly determined from the above experimental data. Using these data we can only calculate the value:

$$\beta\theta^{1/3} \approx 6.95 \times 10^{-2} (\mathrm{sec})^{1/3} . \tag{23}$$

Direct measurement of relaxation time θ in our very dilute polymer solutions is very difficult. One possible way is to evaluate its value using the formula, roughly describing the longest relaxation time in the Rouse model (e.g. see [3], p.222):

$$\theta_R = [\eta]_0 \eta_s M /(N_A k_B T). \tag{24}$$

Here $[\eta]_0$ is intrinsic viscosity whose value ~ 4 is known for the lubricant liquids [11], η_s is the solvent viscosity, M is polymer molecular weight, N_A is Avogadro number, k_B is the Boltzmann constant and T is absolute temperature. At the room temperature, using above values of constants for 0.025% PIB solution in lubricant oil, yields the value $\theta_R \approx 4.54\times10^{-4}$ sec.

Another way of evaluating the relaxation time is hypothesizing that near the sol – gel transition, the polymer concentration in the jet highly increases causing cooperative relaxation effects. Then we can speculate that the transition happens under the condition $We_c = const$ with universal value of We_c. Roughly estimating the critical value $\dot{\varepsilon}_c$ of strain rate in the transition as $\dot{\varepsilon}_c = q/(\pi r_0^2 R)$, results in the relation:

$$We_c = \theta_c \cdot \dot{\varepsilon}_c \approx \theta_c q/(\pi r_0^2 R) = 1/(\pi \nu \beta^3). \tag{25}$$

Using now assumption of universality of We_c, we can utilize the data of papers [7,8], where in case of 0.5% PEO water solution, $\nu_{PEO} = 2.6$ and $\beta_{PEO} = 0.334$, and calculate $We_c \approx 3.3$. Then the value of β in our case where $\nu = 9.7$, is calculated as: $\beta = (\pi \nu We_c)^{-1/3} \approx 0.215$. Substituting this value of β in (22) yields: $\theta_c \approx 3.38\times10^{-2}$ sec. Remarkably, the value of θ_c is almost two orders of magnitude higher than θ_R. In our opinion the value θ_c and related value of parameter β seems preferable. The values of basic constants in equations (21a-c) obtained using fitting procedure, are presented in Table 2.

6. Using open siphon method for evaluation of tackiness of lubricating fluids

As mentioned before the ultimate jet length (or tackiness) strongly depends on the viscosity of oil, molecular weight of dissolved polymer and its concentration in solution. Fig.9 shows the dependence of jet length l on the concentration of PIB with

$M_\eta \approx$ 2,000,000 in two paraffinic oils with respective viscosities 0.068 and 0.022 Pa·sec at 40ºC.

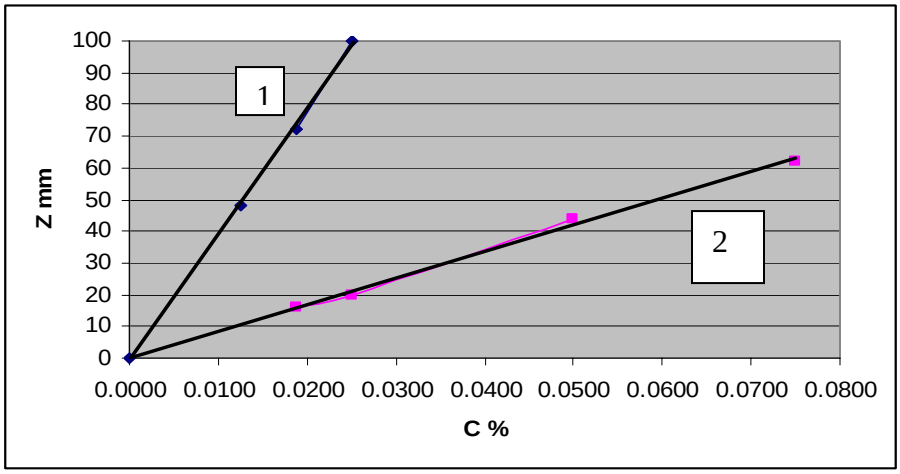

Fig.9. Ultimate jet length l versus the concentration of PIB with $M_\eta \approx$ 2,100,000 in two paraffin oils with respective viscosities 0.068 and 0.022 Pa·sec at 40ºC.

One can see that the dependences of tackiness on polymer concentration in different oils are linear. These dependences are in fact linear for any molecular weight in different oils. It is clear from Fig.9 that decreasing oil viscosity is accompanied by a large decrease in tackiness. For example at the concentration 0.025% of PIB the jet length in oil with viscosity 0.068 Pa·sec is equal to 100 mm, whereas in oil with viscosity 0.022 Pa·sec it is equal 20 mm, i.e. 5 times less than in the first case.

Data presented on Fig.10 demonstrate what the concentration of PIB with different molecular weights in oil with viscosity 0.068 Pa·sec should be used to reach the jet length 100 mm. It is seen that by simply increasing the molecular weight it is possible to substantially increase the tackiness. Increasing molecular weight causes, however, a decrease in both thermal/oxidative stability and shear stability.

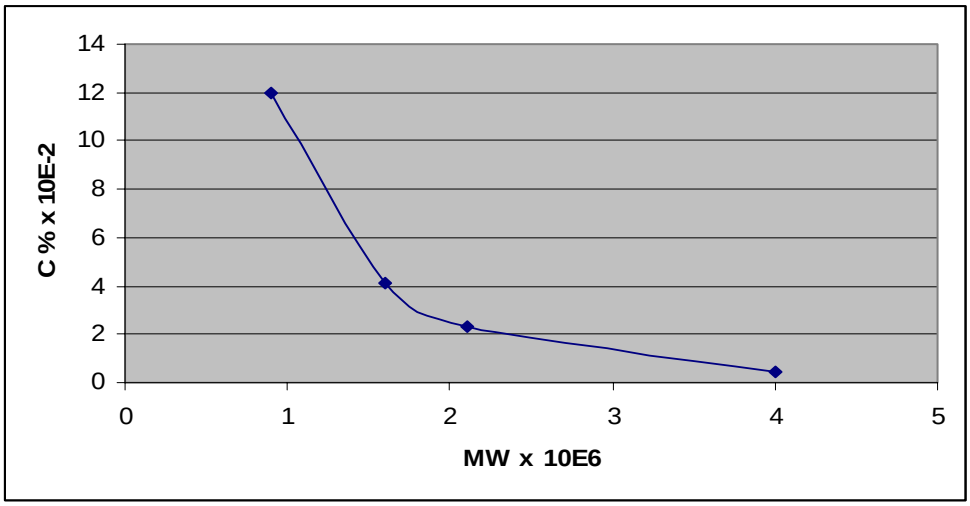

Fig.10. Concentration $C\%$ of PIB in oil with viscosity 0.068 Pa$\cdot$sec corresponding to the jet length $l = 100mm$ versus viscosity average molecular weight M_η of polymer.

Combining the data presented on Figs.9 and 10 it is possible to evaluate the jet length or tackiness for PIB solutions with different molecular weights and at different polymer concentrations.

Unlike PIB's commonly used as tackifiers, the ethylene/propylene copolymers usually do not display tackiness. Nevertheless we obtained some unusual data for the blend of PIB with $M_\eta \approx 2{,}000{,}000$ with very small additive of ethylene/propylene copolymer. Fig.11 demonstrates that adding 0.01% of the copolymer to the PIB solution increases the jet length by about 30%. It should also be mentioned that addition of 0.01% of copolymer to the solution of 0.025% of PIB practically does not change viscosity of the solution. As seen from Fig 11, at higher concentration of the copolymer in PIB solutions the tackiness decreases.

This effect might be explained as follows. Solutions which have 0.01% of copolymer could be considered as very dilute, with macromolecules well separated. During flow induced orientation of long flexible PIB chains, much shorter and more rigid molecules of copolymer are involved in process of orientation and support oriented PIB macromolecules, causing increase in tackiness. With increase in concentration of copolymer, macromolecules form ensembles, which could not be involved in orientation process and moreover could restrict orientation of PIB macromolecules and decrease tackiness.

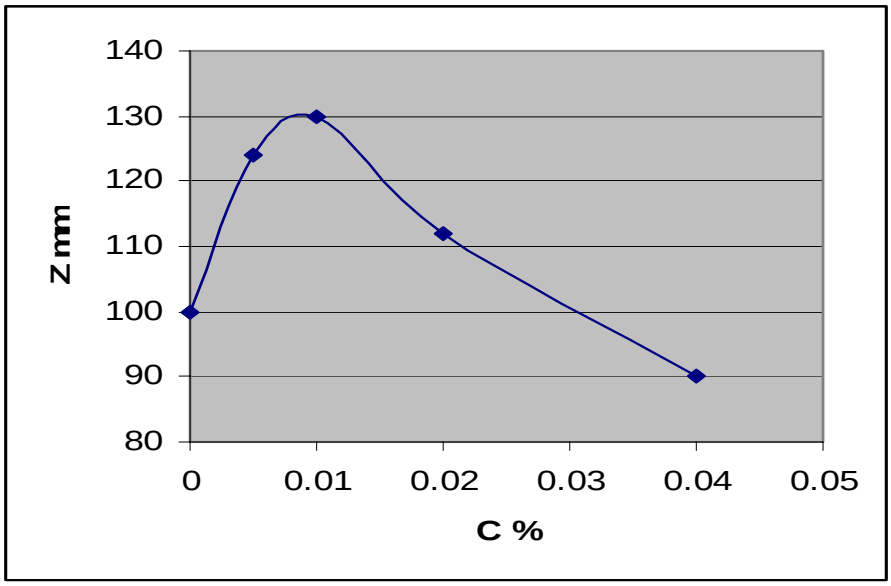

Fig.11. Tackiness effect versus concentration of ethylene/propylene copolymer added to the 0.025% PIB solution in lubricant oil.

7. Conclusions

This paper applies the open siphon method for evaluations of tackiness of several lubricant oils. In these experiments, evacuated sucking tube withdraws vertical free jet of liquids from a jar with a free surface. Dilute solutions of polyisobutelene (PIB) of different molecular weights and polymer concentrations in lubricating fluids, as well as the blends of PIB with ethylene-propylene copolymer were used in these experiments. Time dependences for the length and shape of free jet, and flow rate in the process were recorded in the experiments for several values of vacuum in sucking tube and for several lubricant fluids. The *tackiness* of lubricant fluids was quantified by the ultimate length of free jet just before it breaks up. Several specific phenomena were observed in the experiments, such as solvent exudation out of extended jet, maximum on the time dependence of flow rate during the process, maximum of tackiness for solutions of blends with and with no tackifier, and a two-phase flow in sucking capillary.

Theoretical model developed in this paper is similar to that in paper [8], where the withdrawn jet is treated as a slightly cross-linked elastic gel. The model [8] was modified

in the present paper by including two new features. Firstly we take into account the exudation of the swollen gel under extension, a common effect for dilute polymer solutions, observed in our experiments. Secondly, we made a non-steady extension of an earlier stationary theory [8]. Fitting the theory with experimental data allowed us to well interpret and described the data.

The results of the paper clearly demonstrate that evaluation of tackiness by the open siphon technique presents a simple and reliable method useful for lubricant industry applications.

Acknowledgment

The authors express high gratitude to the president of Functional Products for initiating and supporting this research.

References

1. *Macromolecules* 1 & 2, H.G. Elias Ed., Plenum Press, New York (1984).
2. L.R.G. Treloar, *Physics of Rubber Elasticity*, 3rd ed. Clarendon Press, Oxford (1975).
3. R. G. Larson, *Constitutive Equations for Polymer Melts and Solutions*, Butterworth, Boston (1988).
4. G. Astarita and L. Nicodemo, Extensional flow behavior of polymer solutions, *Chem. Eng. J*., **1**, 57-61 (1970).
5. *The Rheology in Focus*, Elsevier, New York (1993)
6. A. I. Leonov and A. N. Prokunin, *Nonlinear Phenomena in Flows of Viscoelastic Polymer Fluids*, Chapman and Hall, New York (1994), pp106-108, 338-342
7. A.I. Leonov and A.N. Prokunin, On spinnability in viscoelastic liquids. *Trans. Acad. Sci. USSR, Fluid and Gas Mech*., No. 4, 24-33 (1973).
8. A.N. Prokunin, A model of elastic deformation for the description of withdrawal of polymer solutions, *Rheol. Acta*, **22**, 374-379 (1984).
9. L.D. Landau and V.A. Levich , *Acta Phys. Chem. URSS* (Russian) 17, 42 (1942).
10. V.G. Levich, *Physico-Chemical Hydrodynamics* (Russian) Fizmatgiz, Moscow (1959).
11. *Vistanex, Properties and Applications*, Exxon Corporation (1993)
12. *Environmental Contaminate Encyclopedia, Mineral Oils, General Entry*, R.J. Irvin, Editor, July 1, (1997)

Table 1: The values of meniscus variables in the experimental profiles (Fig.8)

q $\mathrm{cm}^3/\mathrm{sec}$	(q_c) 0.03	0.14	0.20	0.25	0.35
r_0 mm	0.216	0.361	0.407	0.438	0.490
R mm	2.10	3.50	3.94	4.25	4.75
$\sigma_0 \times 10^{-2}$ Pa	4.97	5.63	5.98	6.25	6.71
$G_0 \times 10^{-2}$ Pa	6.22	6.38	6.65	6.87	7.26

Table 2: The values of basic constants in equations (21a-c) obtained using fitting procedure

β	ν	$\alpha = \beta\nu$	$m(\nu)$	n	k cm^3/(Pa·sec)	θ sec
0.215	9.7	2.08	14	1,062	2.71×10^{-5}	3.38×10^{-2}

Figure captions

Fig.1. Experimental set up for testing tackiness.

Fig.2a,b. Photographs of free tacky jets for 0.025% PIB solution in lubricant oil.

Fig.3. Schematics of jet withdrawal.

Fig.4. Photographs of two-phase motion of jet in capillary.

Fig.5. Time dependences of flow rate for different vacuum values (shown in the box). 0.025% PIB solution in lubricant oil.

Fig.6. Comparison of time dependences of withdrawal rate $\dot{l}(t)$ (curve 1) and flow rate (curve 2) with vacuum value $\sigma_v = 32KPa$ for 0.025% PIB solution in lubricant oil.

Fig.7. The decreasing branches time dependences of flow rate in Fig.5, represented in semi-logarithmic coordinates.

Fig.8. Jet profiles for several values of flow rate (shown in the box) established by photographing. 0.025% PIB solution in lubricant oil. Symbols – experimental data, solid lines – model calculations.

Fig.9. Ultimate jet length l versus the concentration of PIB with $M_\eta \approx 2{,}100{,}000$ in two paraffin oils with respective viscosities 0.068 and 0.022 Pa·sec at 40ºC.

Fig.10. Concentration $C\%$ of PIB in oil with viscosity 0.068 Pa·sec corresponding to the jet length $l = 100mm$ versus viscosity average molecular weight M_η of polymer.

Fig.11. Tackiness effect versus concentration of ethylene/propylene copolymer added to the 0.025% PIB solution in lubricant oil.